

# **Petrology of Upper Silurian reservoir rocks from the Kudirka Atoll, Lithuania**

On the spatiotemporal relations between different  
diagenetic events that have affected the  
reservoir quality of the rocks

Volume 2(2)

Niels Stentoft, Petras Lapinskas, Petras Musteikis,  
Lars Kristensen and Torsten Hoelstad

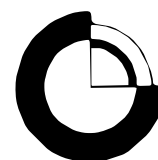


# **Petrology of Upper Silurian reservoir rocks from the Kudirka Atoll, Lithuania**

**On the spatiotemporal relations between different  
diagenetic events that have affected the  
reservoir quality of the rocks**

**Volume 2 (2)**

Niels Stentoft, Petras Lapinskas, Petras Musteikis,  
Lars Kristensen and Torsten Hoelstad



**GEUS**

# Figure legends

**Fig. T-001 - T-199**

## Figure legends

**Fig. T-001.** The limestone of thin section no. 126/1A is a packed biomicrite. The rock is faintly mottled, but it looks very massive, except for some scattered, small vugs (cf. Fig. T-001B). The porous streaks in the red-dyed part of the section are artificially induced by the staining solution (Alizarin S and potassium ferricyanide). Fig. A: plane polarized light; Fig. B: cross polarized light. The thin section is 25 mm in diameter.

**Fig. T-002.** Thin section photomicrograph (plane polarized light) of packed biomicrite. Two ostracod shells are filled with a finegrained geopetal carbonate sediment and a sparry calcite cement. The latter is precipitated in the cavity above the geopetal sediment. The contact between two skeletal grains consist of a microstylolite (grain suturing, lowermost in the picture).

Sample 126/1A. Scale bar equals 300  $\mu\text{m}$ .

**Fig. T-003.** Thin section photomicrograph (plane polarized light). Because of the grain obliterations, the skeletal grain being more or less replaced by micrite/microspar, the rock has an inequigranular, fogged to spotted mosaic fabric. The relatively coarse-grained calcite (C), showing a hypidiotopic fabric, may be a “passive” cement, precipitated in former vugs. Two non-mineralized vugs are seen to the left (P). S is a syntaxial overgrowth on a echinoderm fragment (E).

Sample 126/1A. Scale bar equals 300  $\mu\text{m}$ .

**Fig. T-004.** Ostracod shell with geopetal sediment overlaid by sparry calcite cement. Both the geopetal mud and most of the shell wall have been neomorphic altered, being replaced by an aphanocrystalline to very finely crystalline (Axn - VFxn) xenotopic calcite.

Sample 126/1A. Scale bar equals 50  $\mu\text{m}$ .

**Fig. T-005.** Poorly developed stylolite in an area where the rock has an inequigranular fogged mosaic fabric. Pyrite crystals (Py) are precipitated in the stylolite surface. A faint

solution-enlargement of the stylolite has taken place, cf. Fig. B. Fig. A: plane polarized light; Fig. B: cross polarized light.  
Sample 126/1A. Scale bars equal 100  $\mu\text{m}$ .

**Fig. T-006.** Shows a large calcite crystal (C), which has probably filled up a former solution(?) vug. The calcite inclusions (the arrow) are probably a geopetal sediment, settled to the bottom of the small vug ("crystal silt") before the mineralization of the vug took place. The "string of pearls" of small pyrite crystals (S - S) marks the presence of an "incipient" stylolite. Fig. A: plane polarized light; Fig. B: cross polarized light.  
Sample 126/1A. Scale bars equal 100  $\mu\text{m}$ .

**Fig. T-007.** Photographs of thin section no. 126/2A show a packed biomicrite. The rock contains many small solution vugs, "randomly" scattered. No blue-dyed resin has entered most of these vugs. Fig. A: plane polarized light; Fig. B: cross polarized light. The section is about 25 mm across.

**Fig. T-008.** Thin-section photomicrograph (plane polarized light) showing four rhombohedral dolomite crystals that have replaced both Fxn-Mxn anhedral calcite crystals and the Axn calcite of an almost totally obliterated (by recrystallization) ostracod(?) test. The dolomite crystals are probably stained bluish-green by the alizarin red S and potassium ferricyanide stains due to their content of iron (ferro). A pyrite crystal (Py) is seen in the middle of the picture.  
Sample 126/2A. Scale of bar equals 300  $\mu\text{m}$ .

**Fig. T-009.** Shows an area of the rock section that has an inequigranular, xenotopic fogged mosaic fabric. The irregular, diffuse Axn structures are diagenetic altered fossils. Small scattered pores (P) are seen. The echinoderm fragments (E), probably crinoids, are revealed by their dusty inclusions, embedded in syntaxial calcite cement. Plane polarized light.  
Sample 126/2A. Scale of bar equals 300  $\mu\text{m}$ .

**Fig. T-010.** Thin-section photomicrograph ( $\frac{1}{2}$  crossed nicols) of a brachiopod shell, a little attacked by leaching. The fine-grained calcite crystals above the brachiopod, and in the lower right corner of the picture, have suffered from dissolution - a sieve mosaic fabric is developed here. Sutured grain contacts, or microstylolites (S), are seen between some of the grains, a well-developed one is seen between the coarse-grained syntaxial cement of a crinoid fragment (lowermost in the picture) and the cement crystals precipitated on the one side of the brachiopod shell. Tiny pores are also formed along the microstylolites.  
Sample 126/2A. Scale of bar equals 100  $\mu\text{m}$ .

**Fig. T-011.** Shows an area of the rock rich in dimly outlined moulds from skeletal grains. Several small intercrystalline pores are also seen. The rock has here a sieve mosaic fabric. Plane polarized light.

Sample 126/2A. Scale of bar equals 100  $\mu\text{m}$ .

**Fig. T-012.** Thin-section photomicrograph (plane polarized light) of a bryozoan fragment, probably an oblique section of a fenestrate one. The fibrous microstructure of the thick outer wall and the thin zooecia-walls is obliterated - a micritization has seemingly taken place. Sample 126/2A. Scale bar equals 100  $\mu\text{m}$ .

**Fig. T-013.** Shows four small solution vugs. The vug to the left resembles a mould from a bioclast. Several of the calcite crystals along the walls of the vugs look finely serrated because of the leaching. No calcite cement is precipitated in the vugs. Py is a pyrite grain.  $\frac{1}{2}$ -cross polarized light. Sample 126/2A. Scale of bar equals 100  $\mu\text{m}$ .

**Fig. T-014.** An ostracod filled with sparry calcite cement. Part of the shell wall is dissolved (mouldic porosity). Several tiny solution vugs are seen in the matrix above the ostracod; a relatively large vug is seen in the lower right corner of the picture. Plane polarized light. Sample 126/2A. Scale of bar equals 100  $\mu\text{m}$ .

**Fig. T-015.** A solution vug surrounded by calcite crystals and two subhedral dolomite crystals. The calcite crystals are assuredly affected by the leaching (they are fine-serrated), whereas the dolomite crystals (stained bluish-green) seem to be rather unaffected. However perfect crystal faces towards the vug are not seen at the arrow. Plane polarized light. Sample 126/2A. Scale of bar equals 100  $\mu\text{m}$ .

**Fig. T-016.** Thin-section photographs of sample 126/3B showing a massive limestone, a biosparrudite, which has been strongly dolomitized (the pale blue areas).  
Fig. A: plane polarized light; Fig. B: cross polarized light. The section is 25 mm in diameter.

**Fig. T-017.** Dolomite (being the blue-green stained part) has partly replaced a coarse-grained calcite rock, consisting of crinoids embedded in syntaxial calcite cement. The crinoid fragments are diffuse and appear as dusty inclusions in the cement. The dolomite has a hypidiotopic fabric. Plane polarized light.  
Sample 126/3 B. Scale bar equals 300  $\mu\text{m}$ .

**Fig. T-018.** Poorly preserved shell fragment (brachiopod?) and crinoids embedded in syntaxial cement are partly replaced by dolomite. The dolomite has a hypidiotopic fabric. Note how the staining with Alizarin Red S has made it possible to identify cement zonations: two growth zones are seen in the syntaxial cement (the arrow). Plane polarized light.  
Sample 126/3 B. Scale bar equals 300  $\mu\text{m}$ .

**Fig. T-019.** Thin-section photomicrograph of a crinoid biosparite which has only been faintly dolomitized. Both subhedral and euhedral (rhombohedral) dolomite crystals are seen. Plane polarized light.  
Sample 126/3B. Scale of bar equals 300  $\mu\text{m}$ .

**Fig. T-020.** Thin-section photomicrograph (plane polarized light) of a bryozoan colony being partly replaced by dolomite. The outlines of some of the zooecia are dimly seen as small inclusions in the dolomite crystals. A cement zonation is revealed by the Alizarin Red S stain in the syntaxial cement on the crinoid (arrow), two growth zones (at least) are seen.  
Sample 126/3B. Scale of bar equals 300  $\mu\text{m}$ .

**Fig. T-021.** Thin-section photomicrograph (plane polarized light) of a small solution vug. Both the calcite, a crinoid with syntaxial cement, and the dolomite crystals seem to be attacked by the leaching.  
Sample 126/3B. Scale of bar equals 100  $\mu\text{m}$ .

**Fig. T-022.** Thin-section photomicrograph (plane polarized light) of a trepostome bryozoan colony, partly replaced by dolomite crystals. The diffuse, Axn zooecia walls are partly dissolved.  
Sample 126/3B. Scale of bar equals 300  $\mu\text{m}$ .

**Fig. T-023.** Thin-section photomicrograph (plane polarized light) illustrating three diagenetic steps: a precipitation of syntaxial calcite cement (around a crinoid lowermost in the picture) is followed by precipitation of dolomite (bluish coloured), which in turn is followed by a precipitation of pyrite (cf. the aggregate, built up of small pyrite crystals, uppermost in the picture).  
Sample 126/3B. Scale of bar equals 100  $\mu\text{m}$ .

**Fig. T-024.** Photographs of thin-section no. 131/1B (4 : 1). The rock is a biomicrite. It has some resemblance to a dismicrite (cf. Folk, 1959) as it contains several irregular, longish patches of sparry calcite. However, as most of these structures are arranged with their long axes more and less at right angles to the assumed bedding plane (as indicated by the orientation of longish skeletal fragments, and solution seams), it is assumed that they represent solution-enlarged fractures that have later been filled with sparry calcite (one of the structures is not mineralized). Fig. A: plane polarized light; Fig. B cross polarized light.

**Fig. T-025.** Thin-section photomicrograph (plane polarized light) of biomicrite. The fossils have been more or less replaced by micrite and microspar. The ostracod(?) shell (arrow) is almost ghost-like. Two silica grains (S) and a small dolomite crystal (D) seem to have replaced fine-grained calcite.  
Sample 131/1B. Scale of bar equals 100  $\mu\text{m}$ .

**Fig. T-026.** Thin-section photomicrograph of an almost invisible solution seam. Fig. A: plane polarized light; Fig. B: cross polarized light. A string of pearls of pyrite crystals elucidates the course of the seam. A leaching along the surface of the seam has resulted in the formation of many small pores (Fig. B). Both micrite/microspar and fossils are attacked by the leaching.

Sample 131/1B. Scale of bars equal 100  $\mu\text{m}$ .

**Fig. T-027.** Thin-section photomicrograph (plane polarized light) of packed biomicrite. The rock is here rich in small shell fragments. Geopetal biomicrite overlaid by sparry calcite cement is seen in the ostracod shell (O). E = echinoderm fragments.

Sample 131/1B. Scale of bar equals 300  $\mu\text{m}$ .

**Fig. T-028.** Thin-section photomicrographs of an irregular patch of coarse-grained spar. Fig. A is taken with plane polarized light, Fig. B is taken under blue-light fluorescence. The patch may be a former solution vug that has been filled with calcite cement.

Sample 131/1B. Scale bars equal 300  $\mu\text{m}$  in figure A, and 100  $\mu\text{m}$  in figure B.

**Fig. T-029.** Thin-section photomicrograph of a supposed fracture which has been enlarged by solution, and subsequently filled with sparry cement (A: plane polarized light; B: cross polarized light). A solution seam crosses the structure (S - S). A faint leaching has taken place along the seam (cf. Fig. B). That is the leaching postdates the chemical compaction of the rock.

Sample 131/1B. Scale of bar equals 300  $\mu\text{m}$ .

**Fig. T-030.** Thin-section photomicrographs (half crossed nicols) of fossils that have been partly replaced by micrite. Fig. A shows a shell fragment from a brachiopod which looks as if it has been nibbled by an animal. A bryozoan colony lowermost in the picture is almost totally replaced by micrite. In Fig. B has an echinoderm fragment become very diffuse because of the micrite replacement.

Sample 131/1B. Scale of bars equal 100  $\mu\text{m}$ .

**Fig. T-031.** Photographs (4 : 1) of thin-section no. 131/2B. The rock is a biosparite, rich in crinoid fragments embedded in syntaxial calcite cement. With the naked eye it seems to be massive, except for a part of the section to the right where many small pores are developed in between the grains. A well-developed stylolite is seen to the left. Fig. A: plane polarized light; Fig. B: cross polarized light.

**Fig. T-032.** Thin-section photomicrograph (half crossed nicols) of biosparite. Because of the poor preservation of the fossils (the crinoid fragments being revealed as dusty inclusions, embedded in syntaxial calcite cement) the rock almost shows an inequigranular, xenotopic



fogged mosaic fabric. A few small pores (blue coloured) are seen between the interpetrant grains.

Sample 131/2B. Scale bar equals 300  $\mu\text{m}$ .

**Fig. T-033.** Thin-section photomicrograph (plane polarized light) of a crinoid biosparite. Most of the contacts between the syntaxial calcite cements, that surround the poorly preserved crinoids, consist of microstylolites - the rock has a fitted fabric. Besides the crinoids, a few peloids and a brachiopod fragment (B) are also seen.

Sample 131/2B. Scale of bar equals 300  $\mu\text{m}$ .

**Fig. T-034.** Thin-section photomicrograph (plane polarized light) of fitted grainstone. Virtually all the grain contacts consist of microstylolites that have been solution-enlarged, resulting in the formation of numerous tiny intergranular pores. The nucleation of the scattered sub- to euhedral dolomite crystals (the pale bluish green crystals in the section) seem to have taken place in the microstylolitic grain contacts.

Sample 131/2B. Scale of bar equals 300  $\mu\text{m}$ .

**Fig. T-035.** Thin-section photomicrograph (plane polarized light) of a solution-enlarged stylolite, surrounded by carbonate with fitted fabric, which has also been affected by leaching, as indicated by the small pores formed in the sutured grain contacts. The dolomite crystals (the rhombohedral crystals in the section, that are not stained red by Alizarin Red S) seem only to be very slightly attacked by the corrosive fluids.

Sample 131/2B. Scale of bar equals 100  $\mu\text{m}$ .

**Fig. T-036.** Thin-section photomicrograph (plane polarized light) of a dolomite crystal adjoining a small vug (V) with remains of oil. The vug was formed after the dolomite was precipitated, as indicated by the corroded appearance of the latter.

Sample 131/2B. Scale of bar equals 100  $\mu\text{m}$ .

**Fig. T-037.** Photographs (4 : 1) of thin-section no. 131/3B, show a biosparite with a fitted fabric. Most of the constituent grains are crinoid fragments embedded in syntaxial calcite cement. The rock is very massive; some porosity is, however, developed along the stylolite (cf. Fig. B). Fig. A: plane polarized light; Fig. B: cross polarized light.

**Fig. T-038.** Thin-section photomicrograph (plane polarized light) of interpetrant particles (fitted fabric). The "thin" fracture uppermost is artificially induced. B = bryozoan; Br = brachiopod(?) fragment.

Sample 131/3B. Scale of bar equals 300  $\mu\text{m}$ .

**Fig. T-039.** Thin-section photomicrograph (half crossed nicols) of bryozoan colony. The zooecia walls are diffuse, partly obliterated, due to micritization. Replacing micrite seems also

to have “forced its way” into the intragranular sparry calcite cement (arrows) - the transitions from the zooecia walls to the cements inside the zooecia are very diffuse. Sy is a coarse-grained calcite cement crystal, which has grown syntaxially on the crinoid fragment (E). Sample 131/3B. Scale of bar equals 100  $\mu\text{m}$ .

**Fig. T-040.** Thin-section photomicrographs of a stylolite, forming an interconnected network when seen in cross section (A: half crossed polarized light; B: cross polarized light). Some leaching has definitely taken place along the dentate stylolite surfaces. Most of the grains of the surrounding rock consist of crinoid fragments. Where the intergranular sparry cement has not been totally “cut off” during the chemical compaction, the crinoids appear as dusty inclusions, embedded in the syntaxial cement crystals (arrows). Sample 131/3B. Scale of bars equal 300  $\mu\text{m}$ .

**Fig. T-041.** Thin-section photomicrograph (plane polarized light) of stylolite (another part of the stylolite shown in Fig. T-40). Small pyrite crystals and dolomite rhombohedrals are precipitated in the olive brown insoluble residue accumulation of organic-like matter. Solution has taken place along the stylolite surface. Sample 131/3B. Scale of bar equals 100  $\mu\text{m}$ .

**Fig. T-042.** Photographs (4 : 1) of thin-section no. 131/4B (A: plane polarized light; B: cross polarized light). The massive rock is a biosparite with a well-developed fitted fabric. Two stylolites cross the section. Some dolomitization has taken place: about 1/5 of the rock volume is made up of sub- to euhedral dolomite crystals. The relatively large (pebble-sized) grain to the right is a *Prasopora*-like bryozoan.

**Fig. T-043.** Thin-section photomicrograph (half crossed nicols) of fitted fabric. Small vugs (arrows) are formed in the sutured grain contacts. A phase of leaching postdates pressure solution. The constituent grains are crinoids with syntaxial cements, that have been more or less “cut away” during the chemical compaction of the rock. A crinoid fragment (C) is only revealed by its dusty inclusions, embedded in the syntaxial cement. The shell to the left with the parallel fibrous structure is from a brachiopod. Sample 131/4B. Scale of bar equals 300  $\mu\text{m}$ .

**Fig. T-044.** Thin-section photomicrograph (plane polarized light) of dolomite with hypidiotopic crystallization fabric. The dolomite crystals have replaced surrounding calcite minerals during their growth, residuals of calcite can still be seen inside some of the crystals. Contacts of microstylolites (cf. the grain contacts in Fig. T-43) are *never* developed between adjoining dolomite crystals. Sample 131/4B. Scale of bar equals 300  $\mu\text{m}$ .

**Fig. T-045.** Thin-section photomicrographs (A: plane polarized light; B: cross polarized light) of a coral colony with intraskeletal pores/sparry cement. Arrows point to the same spot

in the two pictures. A phase of leaching has taken place after the cement was precipitated. Small pores are formed in the area between the earlier isopachous, dentate cement and the later more coarse-grained, equant cement innermost in the corallites, but some of the crystals of the latter are also attacked, as intracrystalline pores are formed. Neomorphosis (a micritization) seems to have affected both corallite walls and the dentate cement. The obliteration of the fossils is most clearly seen with the cross polarized light in Fig. B. Sample 131/4B. Scale bars equal 300  $\mu\text{m}$  and 100  $\mu\text{m}$  respectively.

**Fig. T-046.** Thin-section photomicrograph (plane polarized light) of a stylolite with insoluble residue accumulation of organic-like matter. Many tiny pyrite crystals are precipitated in the residue. A phase of leaching with formation of small vugs (V) postdates the pressure solution. Sample 131/4B. Scale bar equals 300  $\mu\text{m}$ .

**Fig. T-047.** Thin-section photomicrographs (plane polarized light) of calcite-replacing dolomite crystals that overlie microstylolites (the arrows). A leaching with formation of small solution vugs (marked with V) postdates the dolomitization. Sample 131/4B. Scale of bars equal 100  $\mu\text{m}$ .

**Fig. T-048.** Photographs (4 : 1) of thin-section no. 131/5A. The rock, a biosparite, shows a well-developed fitted fabric. Scattered, more or less separated, small solution vugs are common (they are stained blue by resin, cf. Fig. A). Less than 5 % of the calcitic rock is replaced by dolomite. The pale bluish dolomite crystals are dimly seen in the Alizarin red S stained part of the section. The constituent grains are crinoid fragments embedded in syntaxial calcite cement. The about 9 mm large fossil in the upper left corner of the picture is a tabulate coral. Fig. A: plane polarized light; Fig. B: cross polarized light.

**Fig. T-049.** Thin-section photomicrograph (plane polarized light) of biosparite with well-developed fitted fabric. Constituent skeletal grains are here crinoid fragments and a bryozoan (to the right). Leaching seems to have taken place along the intergranular microstylolites. Intraskelatal pores are seen in the bryozoan colony. Sample 131/5A. Scale of bar equals 300  $\mu\text{m}$ .

**Fig. T-050.** Thin-section photomicrograph (plane polarized light) of calcite-replacing dolomite crystals. The relatively large crystal in the middle of the picture is superimposed over microstylolites (of the fitted fabric) induced by pressure solution. A part of a poorly preserved bryozoan colony is seen lowermost in the picture. Both zooecia walls and intraskelatal calcite cement seem to have been altered during micritization. A few small dolomite crystals (arrows) are precipitated in the zooecia. A leaching, resulting in formation of small intraskelatal pores, postdates the dolomitization. Sample 131/5A. Scale of bar equals 100  $\mu\text{m}$ .

**Fig. T-051.** Thin-section photomicrographs of small solution vugs (A: plane polarized light; B: cross polarized light). The microstylolitic contacts between the grains are solution-enlarged. The dolomite crystal in the middle of the picture overlies a microstylolite (arrow), indicating that dolomite is contemporaneous with or postdates pressure solution. The presence of tiny pores inside the dolomite (intracrystalline porosity) renders it probable that the solution along the microstylolites postdates dolomitization.  
Sample 131/5A. Scale of bars equal 300  $\mu\text{m}$

**Fig. T-052.** Photographs (4 : 1) of thin-section no. 131/6B show a biosparrudite with granule/pebble sized grains of tabulate coral and stromatoporoid fragments. The rock consist of calcite with about 2 % replacing dolomite. The crystals of the latter are stained pale greyish blue. Four fractures can be discerned: two short solution-enlarged, and two calcite-mineralized crossing the thin-section (arrows). The rock is massive, except for a smaller area around a stylolite (to the right in the picture), where many small vugs form a more or less interconnected pore system. Small isolated areas of intrafossil porosity (in stromatoporoids) are also seen. Fig. A: plane polarized light; Fig. B: cross polarized light.

**Fig. T-053.** Thin-section photomicrograph (plane polarized light) of a stylolite, formed between a tabulate coral with intragranular, neomorphic spar and a recrystallized stromatoporoid colony.  
Sample 131/6B. Scale of bar equals 300  $\mu\text{m}$ .

**Fig. T-054.** Thin-section photomicrograph (cross polarized light) of another part of the stylolite shown in Fig. T-053. The stylolite has here a more complex fabric, forming an interconnected network. A dolomite crystal overlies one of the pressure solution seams, revealed by a string of pearls of tiny pyrite crystals (arrow). A few scattered pyrite crystals are also seen outside the stylolite surfaces, in both calcite and dolomite.  
Sample 131/6B. Scale of bar equals 100  $\mu\text{m}$ .

**Fig. T-055.** Thin-section photomicrographs of biosparite (A: plane polarized light; B: cross polarized light). Due to the poor preservation of fossils the rock has almost an inequigranular fogged mosaic fabric. Neomorphic processes seem to have taken place, as original microstructure of fossils are more and less obliterated, being replaced by micrite and microspar, and the spar around the fossils does not resembles passive cement, as it has a xenotopic fabric, and, more important, sparry calcite has in places replaced fossils; residuals of fossils are seen inside some of the crystals.  
Sample 131/6B. Scale of bars equal 300  $\mu\text{m}$ .

**Fig. T-056.** Thin-section photomicrographs (A: half crossed nicols; B: blue-light fluorescence) of a coarse-grained calcite spar between fossils. Arrows point to same spot in A and B. The spar has a hypidiotopic fabric, showing plane intercrystalline boundaries and an increase of crystal size away from fossil surface (the poorly preserved stromatoporoid uppermost in the picture). These fabrics are usually used as criteria for passively precipitated,

space-filling cement. However, the neomorphic sparry crystals, that have obliterated the original layered structure of the stromatoporoid, are in places observed to overlie the boundary between the stromatoporoid and the coarse-grained intergranular spar (the arrow), indicating that the spar, or at least a part of the spar, below the stromatoporoid has a neomorphic origin. The blue-light fluorescence photograph shown in Fig. B seems to reveal that two generations of cement are present between the fossils: an earlier, rather brightly fluorescent (passive cement probably) which has been obliterated by a later non-fluorescent, neomorphic cement, precipitated contemporaneous with the neomorphic alteration of the fossils.

Sample 131/6B. Scale of bars equal 300  $\mu\text{m}$ .

**Fig. T-057.** Thin-section photomicrograph (plane polarized light) of a stromatoporoid which has been strongly affected by leaching. The original layered boxwork structure of the fossil is preserved to some extent. The calcite-replacing dolomite crystals are also attacked by leaching. However, it is important to stress that some rock solution may also have been caused by the Alizarin red S and potassium ferricyanide stains.

Sample 131/6B. Scale of bar equals 300  $\mu\text{m}$ .

**Fig. T-058.** Thin-section photomicrographs (A: plane polarized light; B: cross polarized light) of a biosparite, taken in an area close to the stylolite (cf. Fig. T-052). Microstylolites are developed around many of the grains (fitted fabric). A rather indistinct fracture crosses the rock, cutting through both fossils (mostly crinoids) and calcite spar. The ghost-like fracture seems to be a mineralized fracture, which has been obliterated during the neomorphic alteration of the rock; it is invisible in cross polarized light (Fig. B).

Sample 131/6B. Scale of bars equal 300  $\mu\text{m}$ .

**Fig. T-059.** Thin-section photomicrograph (plane polarized light) of a fracture, crossing a tabulate coral. The fracture is partly obliterated by neomorphic, xenotopic, intraskeletal spar. Neomorphosis seems also to have affected the skeletal structure: the septae and tabulae of the coral are poorly preserved and diffuse, being almost obliterated in places.

Sample 131/6B. Scale of bar equals 300  $\mu\text{m}$ .

**Fig. T-060.** Photographs (4 : 1) of thin section no. 131/7A show a biosparite, a crinoidal one. One half of the rock section, to the right in the picture, is very massive, whereas the other half contains several small solution vugs, that are formed between the grains in connection with microstylolites (the fitted fabric). Practically all the calcite-replacing dolomite crystals, making up about 5 % of the entire section, are precipitated in the latter half. Fig. A: plane polarized light; Fig. B: cross polarized light.

**Fig. T-061.** Thin-section photomicrographs of crinoid biosparite. Fig. A: From an area of the thin-section with a well-developed fitted fabric. The fossils have here been strongly truncated during pressure solution, and very little sparry cement is preserved. The picture is taken with plane polarized light. Fig. B: From another area of the section where the rock has

not been so strongly affected by pressure solution. The rock is here rich in syntaxial calcite cement. Plane intercrystalline boundaries are in places seen in the coarse-grained spar in this part of the section. The picture is taken with half crossed nicols.  
Sample 131/7A. Scale of bars equal 300  $\mu\text{m}$ .

**Fig. T-062.** Thin-section photomicrograph (plane polarized light) of inter- and intragranular cements. Small scalenohedral cement crystals are precipitated on a brachiopod-like fossil (B), and a syntaxial rimcement on a poorly preserved crinoid (C). Three growth zones are dimly seen in the latter, made visible by the Alizarin red S stain: I, II and III. The isopachous cement, being scalenohedral in habit, is precipitated before the syntaxial cement on the crinoid, at least before cement generation II and III were precipitated. Microstylolites are developed in grain contacts during a phase of pressure solution (arrows). The pressure solution was followed by a phase of leaching, resulting in the formation of small intergranular vugs. The fact that a microstylolite forms a part of the wall of some of the solution vugs makes it inconceivably, that a dissolution of the rock took place before the pressure solution. The pores marked P in the picture may represent original intra- and intergranular pores, that have only been enlarged very little during the later leaching of the rock.  
Sample 131/7A. Scale of bar equals 100  $\mu\text{m}$ .

**Fig. T-063.** Thin-section photomicrograph (plane polarized light) of dolomite crystals, that are observed to overlie pressure solution seams formed between crinoids. A few small pores (in the lower left corner of the figure) postdate the pressure solution: they are formed immediately along the seams.  
Sample 131/7A. Scale of bar equals 100  $\mu\text{m}$ .

**Fig. T-064** Thin-section microphotographs showing growth-zones in syntaxial cement. Fig. A: With the use of plane polarized light two growth-zones are dimly seen: I and II. Fig. B: Two growth-zones are distinctly illuminated with use of blue-light fluorescence: a brightly fluorescent earlier generation, forming a thin "border" around the crinoids, and a non-fluorescent later generation occupying most of the intergranular spaces. Note that it is not exactly the same two growth-zones that are illuminated in the two photographs.  
Sample 131/7A. Scale of bars equal 300  $\mu\text{m}$ .

**Fig. T-065.** Photographs (4 : 1) of thin-section no. 131/8B showing a biosparite to biosparrudite with fitted fabric. Granule/pebble sized grains are coral and stromatoporoid fragments. The very massive calcite rock is faintly dolomitized (3 - 5 %). The calcite-replacing dolomite crystals appear as pale bluish grains in the Alizarin red S stained part of the section (Fig. A), they are nucleated between the calcite grains, in connection with the microstylolitic grain contacts. The few, rather large, opaque and angular grains are pyrite crystals. Fig. A: plane polarized light; Fig. B: cross polarized light.

**Fig. T-066.** Thin-section photomicrographs of biosparite with fitted fabric. The constituent grains are crinoids and bryozoams. A silica grain of unknown origin is also seen, showing

pseudo-uniaxial cross between crossed nicols. The photo is taken in a small area of the section, being relatively rich in small solution vugs (arrows). Note how the microstylolites between the grains have been solution-enlarged here and there. Fig. A is taken in plane polarized light, Fig. B in cross polarized.  
Sample 131/8B. Scale of bars equal 300  $\mu\text{m}$ .

**Fig. T-067.** Thin-section photomicrograph (half-cross polarized light) shows a crinoid fragment and another fossil (bryozoan?). They are both very poorly preserved, note the diffuse outlines. The intergranular cement consist of syntaxial cement (S) and sparry cement with a xenotopic fabric (X). The latter may be neomorphic spar formed contemporaneous with the neomorphic alteration of the bryozoan(?). The isopachous cement between the syntaxial cement and the bryozoan(?) (arrow) may either be an original isopachous cement, which has partly survived the diagenetic alteration of the rock, or it may be a former isopachous cement, neomorphic altered together with the original skeletal microstructure.  
Sample 131/8B. Scale of bar equals 100  $\mu\text{m}$ .

**Fig. T-068.** Thin-section photomicrograph (plane polarized light) of a tabulate coral. The skeletal structure of both tabulae and tube walls is to some extent obliterated. Some of the crystals of the intraskeletal spar, that show a xenotopic fabric, are super imposed over tabulae, indicating that the spar is a neomorphic cement. The fine-grained, porous carbonate uppermost in the picture has some resemblance to "crystal silt".  
Sample 131/8B. Scale of bar equals 300  $\mu\text{m}$ .

**Fig. T-069.** Photographs (4 : 1) of thin-section no. 132/1 B show a rather porous biosparrudite. granule-pebble sized allochems are stromatoporoids and corals. The rock has a fitted fabric. A leaching has taken place via the microstylolites - they have been strongly solution-enlarged in many places. Several intraskeletal pores are also seen. Fig. A is taken with plane polarized light; Fig. B with cross polarized light.

**Fig. T-070.** Thin-section photomicrographs of a tabulate coral. Both corallite wall and tabula look blurred in plane polarized light (Fig. A) due to micritization. An isopachous cement, scalenohedral in habit, is dimly seen. The contacts between this cement and the coarse intraskeletal, xenotopic spar are not sharp. The isopachous cement becomes a little more distinct in cross polarized light (Fig. B), but it is still impossible to point out the contacts between skeletal wall and cement. It seems as if both skeleton and isopachous cement have been micritized. The distal part of the isopachous cement crystals looks ragged: it seems to have been obliterated during the precipitation of the coarse equant cement. With fluorescence microscopy (Fig. C) seems it possible to delineate more clearly the distribution of the brightly fluorescent skeleton with (earlier) isopachous calcite and non-fluorescent (burial) equant calcite (EC). However, the contacts between isopachous cement and fossil are indistinct (the arrows).  
Sample 132/1 B. Scale of bars equal 100  $\mu\text{m}$ .

**Fig. T-071.** Thin-section photomicrograph (plane polarized light) of poorly preserved fossils. The bryozoan zooecia are blurred by micritization, and truncated by pressure solution. E = echinoid fragment; SC = syntaxial cement; MS = microstylolite; D = dolomite. Sample 132/1B. Scale of bar equals 100  $\mu\text{m}$ .

**Fig. T-072.** Thin-section photomicrograph of fitted fabric. A leaching phase postdates pressure solution. Surfaces of microstylolites are solution-enlarged, and preexisting(?) intragranular pores, in the bryozoans, are enlarged. Sample 132/1B. Scale of bar equals 300  $\mu\text{m}$ .

**Fig. T-073.** Thin-section photomicrograph of dolomite rhombohedrals that are superimposed over microstylolites, indicating that dolomitization is contemporaneous with or postdates pressure solution. Sample 139/1B. Scale of bar equals 100  $\mu\text{m}$ .

**Fig. T-074.** Photographs (4 : 1) of thin-section no. 132/2B showing a rather porous biosparrudite (it resembles the rock of sample 132/1B). Granule-pebble sized grains are stromatoporoid and coral fragments. Note that the fitted fabric is still distinct even a dissolution has taken place after the pressure solution. Fig. A: plane polarized light; Fig. B: cross polarized light.

**Fig. T-075.** Thin-section photomicrograph (plane polarized light) of massive rock with fitted fabric. Most allochems are poorly preserved crinoids with syntaxial calcite cements, that have been more or less truncated during the chemical compaction of the rock. Small rhombohedral dolomite crystals are nucleated in the microstylolitic grain contacts (arrows). Tiny solution vugs (P) are also formed here, directly in contact with the seams. Sample 132/2B. Scale of bar equals 300  $\mu\text{m}$ .

**Fig. T-076.** Thin-section microphotograph (plane polarized light) of porous rock with many intergranular and intercrystalline pores. Intragranular pores are seen to the right in the figure, in a stromatoporoid-like fossil. The microstylolites between the grains have been solution-enlarged in many places. Both fossils and spar are attacked by leaching, but skeleton structures, built up of small crystals are relatively most corroded. Some of the small, scattered rhombohedral dolomite crystals (arrows) are also attacked by leaching. Sample 132/2B. Scale of bar equals 300  $\mu\text{m}$ .

**Fig. T-077.** Thin-section photomicrograph (A: plane polarized light; B: cross polarized light) of a bryozoan with almost obliterated zooecia walls. Both the walls and the intragranular carbonate have got a dusty, gritty appearance, they seem to be built up of micrite. However, with cross polarized light (Fig. B), a rather indistinct, almost blurred, sutured mosaic fabric



appears. The rock seems to be Fxn-Mxn, with an anhedral crystallization texture. Perhaps an aggrading neomorphism has started.

Sample 132/2B. Scale of bars equal 100  $\mu\text{m}$ .

**Fig. T-078.** Photographs (4 : 1) of thin-section no. 132/3B show a *Favosites*-like coral, with corallites partly filled with blocky cement. Blue-dyed resin has only entered the intraskeletal pores near the plug surface. A stylolite with yellowish brown insoluble residue accumulation is formed in the contact between the coral and a stromatoporoid-like grain (to the left in the figure). C marks an area of the section consisting of crinoids (with fitted fabric) that has been strongly dolomitized. The dolomite crystals are stained pale blue by Alizarin red S.

Fig. A is taken with plane polarized light, Fig. B with cross polarized light.

**Fig. T-079.** Thin-section photomicrographs of an oblique section through tabulate coral (Fig. A: plane polarized light; Fig. B: half-cross polarized light). The “fuzzy”, fibrous wall structure, with a median dark line, is still preserved. A tabula (T) and several spine-like septae (S) are also seen. The corallites are filled with a hypidiotopic spar, perhaps a “passive” cement. The size of the cement crystals increases away from the skeletal surfaces. However, the contacts between the fossil and the spar are not sharp and well-defined. A close-up of the the coralite wall (Fig. B) seems to show that an incipient aggrading neomorphism has taken place: lobate to serrated outlines of blurred crystals can be dimly seen (arrows).

Sample 132/3B. Scale of bars equal 300  $\mu\text{m}$  and 100  $\mu\text{m}$  respectively.

**Fig. T-080.** Thin-section microphotograph (plane polarized light) of stylolites - a well-developed one and several microstylolites - between crinoids (E), tabulate coral (Co), and stromatoporoid(?) (St). A phase of leaching postdates pressure solution. Note that some of the small pores are in directly contact with surface of microstylolites.

Sample 132/3B. Scale of bar equals 300  $\mu\text{m}$ .

**Fig. T-081.** Photographs (4 : 1) of sample 132/4B: Fig. A with plane polarized light, and Fig. B with cross polarized light. They show a trasverse -oblique section through part of a stromatoporoid colony. The concentric laminae and pillars are indistinct and blurred. The more and less sparfilled, longish vugs resemble fenestral pores. They are probably formed during the growth of the colony. Arrows point to spots that are microphotographed, Cf Fig. T-083 and T-084.

**Fig. T-082.** Thin-section microphotographs (A: plane polarized light; B: cross polarized light) of part of a stromatoporoid colony. Laminae and pillars are “ghost”-like, being revealed by dusty inclusions embedded in smaller calcite crystals. The skeleton is almost invisible between crossed polars (Fig. B). The stromatoporoid seems to have been altered by an aggrading neomorphism, resulting in an inequigranular, xenotopic, sutured mosaic fabric of the rock.

Sample 132/4B. Scale of bars equal 300  $\mu\text{m}$ .

**Fig. T-083.** Thin-section microphotograph (plane polarized light) of a part of a fenestral-like pore in the stromatoporoid, which is partly occupied by a coarse-grained calcite spar, rhombohedral in habit. The spar shows plane intercrystalline boundaries with crystal-face junctions (arrows).

Sample 132/4B. Scale of bar equals 300µm.

**Fig. T-084.** Thin-section microphotograph (plane polarized light) showing intergranular and intercrystalline porosity, formed by solution-enlargement of the microstylolites, that surround the grains (fitted fabric). The syntaxial cement around crinoids (Cr) is truncated by the pressure solution. St = stromatoporoid, altered by an aggrading neomorphosis. Several small euhedral dolomite crystals (D) are precipitated in insoluble residue accumulations of microstylolites.

Sample 132/4B. Scale of bar equals 300 µm.

**Fig. T-085.** Photographs (4 : 1) of vuggy biolithite with subordinate crinoid biosparite (A: plane polarized light; B: cross polarized light). A part of a stromatoporoid colony makes up more than the half of the section. A crinoid biosparite with fitted fabric is seen to the left, and a tabulate coral lowermost. The two porous areas (A), being more and less surrounded by parts of the stromatoporoid colony, are rich in sub- to euhedral dolomite crystals and indeterminable shell fragments. Arrows point to areas that have been microphotographed, cf. Fig. T-086 - T-89.

Sample 132/5B.

**Fig. T-086.** Thin-section microphotograph (plane polarized light) of biosparite with fitted fabric. A phase of leaching, with formation of small intergranular pores, postdates pressure solution. The pale blue crystals are calcite-replacing dolomite, precipitated contemporaneous with or after the pressure solution.

Sample 132/5B. Scale of bar equals 300 µm.

**Fig. T-087.** Thin-section microphotograph (plane polarized light) of a primitive, wave-like stylolite with yellowish brown insoluble residue accumulations, formed between biosparite stromatoporoid colony (in the upper part of the picture). A fitted fabric was formed in the former during the pressure solution. Small solution-vugs were formed later on. Note that the skeletal structure, with laminae and pillars, of the stromatoporoid is obliterated: an aggrading neomorphism seems to have taken place.

Sample 132/ 5B. Scale of bar equals 300 µm.

**Fig. T-088.** Thin-section microphotograph (plane polarized light) of part of a 1 × ½ cm large porous rock with sieve mosaic fabric, embedded in stromatoporoid colony (cf. Fig. T-085). Both skeletal grains and dolomite euhedrals are attacked by leaching. Isopachous cements on shell fragments seem to be neomorphic altered together with the shells themselves (arrows).

Sample 13 2/5B. Scale of bar equals 300  $\mu\text{m}$ .

**Fig. T-089.** Thin-section microphotograph (plane polarized light) of part of stromatoporoid with two dissolution structures (the relatively dark-coloured,  $\text{Axn-VFxn}$  calcite strings), that are assumed to be incipient solution seams. Sub- to euhedral dolomite crystals are observed to overlie the structures.

Sample 13 2/5B. Scale of bar equals 300  $\mu\text{m}$ .

**Fig. T-090.** Photographs (4 : 1) of packed biomicrudite, with granule/pebble sized grains of stromatoporoid colonies. The rock is massive, and seems to be impervious to pore fluids. Geopetal sediments in former shelter-pores indicate that the section is, accidentally, almost placed in the correct position in proportion to the top to bottom relation of the rock, at the time the geopetal sediment was lithified. Arrows point to areas of the section that have been microphotographed, cf. Fig. T-091 - T-093.

Figure A is taken with plane polarized light, figure B with cross polarized light.

Sample 135/1B.

**Fig. T-091.** Thin-section photomicrograph of packed biomicrite (cross polarized light). Note the almost ghost-like appearance of the fossils. Some replacement by micrite has definitely taken place.

Sample 135/1B. Scale of bar equals 300  $\mu\text{m}$ .

**Fig. T-092.** Thin-section microphotographs of geopetal biomicrite in former voids formed by the shelter effect of skeletal grains (trilobite shell fragments). The pore spaces between the geopetal sediments and the skeletal grains are occupied by sparry calcite. The skeletal microstructure of the trilobites is obliterated by neomorphic micrite. Note the indistinct contact between trilobite shell and overlaying micrite in Fig. A. Some of the syntaxial, isopachous cement crystals on this shell are still visible. Fig. A: cross polarized light; Fig. B: plane polarized light.

Sample 135/1B. Scale of bars equal 300  $\mu\text{m}$ .

**Fig. T-093.** Thin-section microphotograph (plane polarized light) of a stylolite, partly formed between a stromatoporoid (lowermost in the picture) and biomicrite. The stylolite seam has been partly solution-enlarged; note the small pores marked with arrows.

Sample 13 5/1B. Scale of bar equals 300  $\mu\text{m}$ .

**Fig. T-094.** Photographs (4 : 1) of biolithite, probably oblique section through part of a stromatoporoid colony, which has been altered by an aggrading neomorphism. The rock is massive, not a single little pore was observed. Fig. A: plane polarized light; Fig. B: cross polarized light.

Sample 135/2B.

**Fig. T-095.** Thin-section microphotographs (A: plane polarized light; B: cross polarized light) of an assumed stromatoporoid colony that has been neomorphic altered. No sign of laminae and pillars are left. Under crossed nicols (Fig. A) the rock is observed to have an equigranular, xenotopic, sutured mosaic fabric, the longish calcite crystals being arranged with their long axes parallel to each other.

Sample 135/2B. Scale of bars equal 300  $\mu\text{m}$ .

**Fig. T-096.** Shows a blue-light fluorescence photograph of a part of a stromatoporoid colony. No skeletal structures become obvious using fluorescence microscopy.

Sample 135/2B. Scale of bar equals 50  $\mu\text{m}$ .

**Fig. T-097.** Photographs (4 : 1) of sample 135/3B showing either a biomicrudite or a biolithite with infiltrated skeletal mud (biomicrite now). A transverse section through part of a stromatoporoid colony is seen to the left, a fossiliferous to spars biomicrite (Bm) with subordinate biosparite (Bs) to the right. A sparfilled vug is seen in the bottom right-hand corner. Arrows point to areas that have been microphotographed (Fig. T-100 and T-101). Sparfilled shelter pores, beneath fossils, indicate that original direction to the top of the rock was to the left in the figures. Fig. A: plane polarized light; Fig. B: cross polarized light.

**Fig. T-098.** Thin-section microphotograph (plane polarized light) of matrix of biomicrite. The original lime mud has been neomorphic altered, and shows now a sutured mosaic of Axn-Vfxn anhedral calcite crystals. The fossils have been more and less replaced by the same aphanocrystalline to very finely crystalline calcite.

Sample 135/3B. Scale of bar equals 50  $\mu\text{m}$ .

**Fig. T-099.** Thin-section microphotograph (plane polarized light) of biosparite (cf. Fig. T-097). Note the very poor state of preservation of crinoids and other fossils.

Sample 135/3B. Scale of bar equals 300  $\mu\text{m}$ .

**Fig. T-100.** Thin-section microphotograph (plane polarized light) showing the boundary between stromatoporoid colony (lowermost) and biomicrite. The aggrading neomorphism of the stromatoporoid may either have spread into the micrite, or contrary, the micritization of biomicrite may have spread into the neomorphic altered stromatoporoid. Two small pores are seen in the latter.

Sample 135/3B. Scale of bar equals 100  $\mu\text{m}$ .

**Fig. T-101.** Thin-section photomicrograph (plane polarized light) of a coarse-grained spar (to the right in the picture), probably precipitated in a former vug in biomicritic rock. A gradual transition in the size of calcite crystals is seen between the micrite, farthest to the left in the picture, and the sparry cement. The contact between rock matrix and cement has been

blurred by recrystallization, only the dusty inclusions in the crystals of the matrix seem to reveal the position of the wall of the former vug (the arrow).

Sample 135/3B. Scale of bar equals 300  $\mu\text{m}$ .

**Fig. T-102.** Thin-section photographs (4 : 1) of sample 135/4B. The rock consists of stromatoporoid colonies, with biomicrite in between. We are dealing with either a biomicrudite or a biolithite with infiltrated skeletal lime mud that has been altered to biomicrite (cf. sample 135/3B). Geopetal biomicrite (in fossils) shows that the original direction to the sediment top is downwards in the picture. Arrows point to areas where the microphotographs T-104 and T-105 are taken. Note that the biomicrite contains some dismicrite-like structures. A is taken with plane polarized light, B with cross polarized light.

**Fig. T-103.** Thin-section photomicrograph (plane polarized light) of the matrix of the biomicrite. A fossil, perhaps an ostracod shell fragment, is ghost-like because of micrite replacement. Indistinct outlines of very finely crystalline calcite crystals indicate that an aggrading neomorphism of the micrite has taken place.

Sample 135/4B. Scale of bar equals 50  $\mu\text{m}$ .

**Fig. T-104.** Thin-section photomicrograph (plane polarized light) of one of the irregular patches of sparry calcite in the biomicrite, that resemble dismicritic spar patches. A spar-filled ostracod shell is seen inside the structure.

Sample 135/4B. Scale of bar equals 300  $\mu\text{m}$ .

**Fig. T-105.** Thin-section photomicrographs (A: plane polarized light; B: cross polarized light) showing the boundary between part of stromatoporoid colony (lowermost in the picture) and biomicrite. Note the lobate to serrate outline of the stromatoporoid. The outer part of the colony seems to have been partly replaced by micrite.

Sample 135/4B. Scale of bars equal 300  $\mu\text{m}$ .

**Fig. T-106.** Thin-section photographs (4: 1) of biosparrudite, with granule/pebble sized grains of fragmented crinoids and stromatoporoids. Most of the spar is syntaxial rimcement on crinoids. The microstylolites in the grain contacts (fitted fabric) are attacked by leaching, and several zig-zagging, fracture-like pores are formed. No blue-dyed resin has entered these small, narrow pores. Fig. A: plane polarized light; Fig. B: cross polarized light.

Sample 135/5B.

**Fig. T-107.** Thin-section photomicrograph (plane polarized light) of biosparite. The fossils (crinoids and bryozoans) are poorly preserved. The crinoids appear as dusty inclusions, embedded in syntaxial cement. The latter has confined the bryozoan fragments. It looks as if syntaxial cement has partly replaced the bryozoan zooecia walls (arrow). The intergranular rimcement shows both plane and microstylolitic intercrystalline boundaries, the latter being formed during a phase of pressure solution.

Sample 135/5B. Scale of bar equals 300  $\mu\text{m}$ .

**Fig. T-108.** Thin-section photomicrographs (A: plane polarized light; B: cross polarized light) of a shell filled with geopetal calcite sediment. The shell resembles an ostracod, but as it shows an indistinct fibrous shell structure, running subparallel to the outer margin of the shell, it may rather be a brachiopod shell. Note the indistinct outlines of the shell itself. Two cement-generations, an earlier scalenohedral and a later rhombohedral, seem to have been precipitated in a former shelter pore beneath the shell, but the contact between the two generations is blurred. The cement of both generations seem to have grown partly at the expense of a bryozoan (arrow). The echinoderm fragment (E) inside the geopetal sediment is not surrounded by syntaxial cement, like the fragments above the sediment, but it is on the contrary partly replaced by micrite (Fig. B).

Sample 135/5B. Scale of bars equal 300  $\mu\text{m}$ .

**Fig. T-109.** Thin-section photographs (4 : 1) of biosparrudite with granule/pebble sized grains of stromatoporoid fragments. By volume is most of the spar of the rock syntaxial calcite cement, precipitated on crinoid fragments. The rock has a fitted fabric. The microstylolites between grains are enlarged a little by dissolution. None of the small vugs, formed here, are filled with blue-dyed resin.

Fig. A: plane polarized light; Fig. B: crosspolarized light.

Sample 135/6B.

**Fig. T-110.** Thin-section photomicrographs (plane polarized light) of biosparite with fitted fabric. All the boundaries between the grains shown in Fig. A consist of microstylolites. Most of the grains are crinoid fragments, embedded in syntaxial cement. A more well-developed, dentate surface is developed, during the pressure solution, between biosparite and a large fossil, a recrystallized stromatoporoid colony, cf. Fig. B. This stylolite has rather high amplitudes, when seen in cross section, and contains yellowish brown insoluble residue accumulations. Small solution vugs along the stylolite surface (arrows) postdate the pressure solution.

Sample 135/6B. Scale of bars equal 300  $\mu\text{m}$ .

**Fig. T-111.** Thin-section photographs (4 : 1) of sample 135/7B (taken with plane polarized light and cross polarized light respectively). They show a massive biosparite. However, a small area of the section (to the right in the figures) consist of a packed biomicrite. A dismicrite-like structure of spar is seen in the latter. Most grains of the rock are crinoid fragments, embedded in syntaxial spar.

**Fig. T-112.** Thin-section photomicrograph (plane polarized light) of biosparite, or perhaps more correctly biopelsparite, with poorly preserved fossils of crinoids and indeterminable shell fragments. A small coralline alga is seen in the upper left corner of the picture.

Sample 135/7B. Scale of bar equals 300  $\mu\text{m}$ .

**Fig. T-113.** Thin-section photomicrographs (A: cross polarized light; B: plane polarized light) of packed biomicrite. Note the serrated boundary between fossils and matrix. A micritization seems to have affected the fossils. Fig. B is a close-up of the rock from the same area. It shows, perhaps, a fossil that has been totally obliterated because of micritization (cf. the diagenetic considerations in the description of the thin-section). Sample 135/7B. Scale of bar equals 300  $\mu\text{m}$  in Fig. A, and 50  $\mu\text{m}$  in Fig. B.

**Fig. T-114.** Thin-section photomicrograph of a small part of a rather indistinct stylolite in a biosparite. The grains consist of crinoids, appearing as dusty inclusions, embedded in syntaxial cement, and peloids. The latter are probably fossil fragments that have been replaced by micrite. Tiny pores are formed in the seam (arrows). D is a small rhombohedral of dolomite. Sample 135/7B. Scale of bar equals 100  $\mu\text{m}$ .

**Fig. T-115.** Thin-section photographs (4 : 1) of sample 135/8B. A: plane polarized light; B: cross polarized light. The rock is a massive biosparite with granules of stromatoporoid fragments. Most of the intergranular spar consist of syntaxial cement on crinoid fragments.

**Fig. T-116.** Thin-section photomicrograph (plane polarized light) of biosparite with very poorly preserved fossils. They have been more and less replaced by micrite, but truncations have also in places taken place by sparry calcite crystals. Note that the intercrystalline boundaries of the spar are irregular, being lobate to serrate. Sample 135/8B. Scale of bar equals 300  $\mu\text{m}$ .

**Fig. T-117.** Thin-section photomicrograph (plane polarized light) of intergranular spar with a small pore. The boundaries between spar and fossils are very indistinct. Ghosts of isopachous cement, probably scalenohedral in habit, are seen on fossils (arrows). The pore may represent a small remains of an original cavity that has never been occupied by cement. Sample 135/8B. Scale of bar equals 300  $\mu\text{m}$ .

**Fig. T-118.** Fig. A shows a thin-section photomicrograph, taken with cross polarized light, of intergranular sparry calcite, precipitated between a brachiopod shell fragment and crinoid fragments. The syntaxial cement around one of the crinoids is seen to the left (the dark area). The skeletal microstructure of the brachiopod is obliterated, but a parallel fibrous structure, running sub-parallel to the margin of the shell, can still dimly be seen. The contact between shell and cement is very indistinct, but an isopachous earlier generation of cement of finer dentate crystals (scalenohedrals) are vaguely seen between the blocky spar and the shell. Arrow points to same spot in Fig. B, which is a close-up of the blurred boundary between spar and brachiopod shell. The photograph is here taken with half-cross polarized light. Sample 135/8B. Scale of bars equal 100  $\mu\text{m}$  and 50  $\mu\text{m}$  respectively.

**Fig. T-119.** Thin-section photographs (4 : 1) of sample 13 5/9B show a massive, packed biomicrite. No syntaxial calcite cement surrounds the crinoid fragments, that make up a great part of the allochems. Some leaching has taken place along the stylolite surfaces (cf. Fig. B). Fig. A: plane polarized light; Fig. B: cross polarized light.

**Fig. T-120.** Thin-section photomicrograph (cross polarized light) of a silica crystal (arrow), three rhombohedral dolomite crystals, and an opaque crystal, probably of pyrite, that all seem to have been nucleated in the micrite matrix of the biomicrite.  
Sample 13 5/9B. Scale of bar equals 50  $\mu\text{m}$ .

**Fig. T-121.** Thin-section photomicrograph (plane polarized light) of biomicrite. A solution-enlarged, wavy stylolite crosses the picture from left to right. Several tiny pyrite crystals are precipitated in micrite matrix and fossils. A sparfilled bryozoan and a echinoderm fragment are seen among the fossils, that have all been replaced somewhat by micrite; note the “ragged” outline of the fossils. P = pore.  
Sample 13 5/9B. Scale of bar equals 300  $\mu\text{m}$ .

**Fig. T-122.** Thin-section photomicrograph (plane polarized light) of the fine-grained rock matrix. It is built up of Axn-VFxn calcite, and has a xenotopic sutured mosaic fabric.  
Sample 13 5/9B. Scale of bar equals 50  $\mu\text{m}$ .

**Fig. T-123.** Thin-section photographs (4 : 1) of sample 135/10B show a packed to sparse biomicrudite. The rock resembles that of sample 135/9B, but it has a mottled appearance as if it has been bioturbated before it got lithified. Arrow points to a dismicrite-like sparry structure, cf. Fig. T-125. The direction to top of sediment before it become lithified is also shown. Fig. A: plane polarized light; Fig. B: cross polarized light.

**Fig. T-124.** Thin-section photomicrograph (plane polarized light) of biomicrite. Note the indistinct, “blurred” contacts between fossils and matrix. Micrite-replacements of skeletons have taken place; only the intragranular sparry cement is left of the ostracod(?), marked by an arrow.  
Sample 135/10B. Scale of bar equals 300  $\mu\text{m}$ .

**Fig. T-125.** Thin-section photomicrograph (plane polarized light) of part of a dismicrite-like sparry body. The contact between spar and surrounding micrite matrix is not sharp, and the spar itself has a xenotopic sutured mosaic fabric. Therefore, it is possible that the spar represents a former “passive” cement that has been neomorphic altered contemporaneous with the recrystallization of the muddy rock matrix. Geopetal micrite is seen inside an ostracod shell.  
Sample 135/10B. Scale of bar equals 300  $\mu\text{m}$ .



**Fig. T-126.** Thin-section photomicrograph (plane polarized light) showing a stylolite which has been solution-enlarged. Note the poor preservation of the fossils: echinoderms, brachiopod, bryozoan and other indeterminable shell fragments. Sample 135/10 B. Scale of bar equals 300  $\mu\text{m}$ .

**Fig. T-127.** Thin-section photographs (4 : 1) of sample 135/11 B show a packed biosparrudite to biomicrudite. The massive rock has a fitted fabric. Arrows point to solution-enlarged stylolite and sparfilled shelter pore beneath a brachiopod shell, cf.. Fig. T-129 and T-128.

A: plane polarized light; B: cross polarized light.

**Fig. T-128.** Thin-section photomicrograph (plane polarized light) of sparry calcitr beneath a brachiopod shell, probably occupying a former shelter pore. The upper surface of the brachiopod shell is blurred - it looks as if the recrystallization of the overlaying lime mud has spread into the shell. Note that the boundaries are also blurred between spar and underlaying microsparite, and between microsparite and bryozoan colony.

Sample 135/11 B. Scale of bar equals 300  $\mu\text{m}$ .

**Fig. T-129.** Thin-section photomicrograph (plane polarized light) of solution-enlarged stylolite. Microstylolitic grain contacts are seen between the grains (bryozoans, brachiopods and echinoderms); small sub- to euhedral, calcite-replacing dolomite crystals are precipitated here (arrows).

Sample 135/11 B. Scale of bar equals 300  $\mu\text{m}$ .

**Fig. T-130.** Photographs (4 : 1) of thin-section 136/1 B showing a rather massive biosparrudite, or rather a biolithite with some biosparrudite, because a part of a coral (*Favosites*?) makes up more than the half of the section. All the pores of the rock are connected to the area outside the large coral, where they are formed by a solution-enlargement of microstylolites between the grains. Arrows point to porous areas shown in Fig. T-131 and T-132.

A: plane polarized light; B: cross polarized light.

**Fig. T-131.** Thin-section photomicrograph (plane polarized light) of biosparite. Note the poor state of preservation of the fossils, they have been truncated during a chemical compaction, but obliterations of the skeletal structures by replacing micrite seem also to play a part.

Sample 136/1 B. Scale of bar equals 300  $\mu\text{m}$ .

**Fig. T-132.** Thin-section photomicrographs (plane polarized light) of intergranular pores, formed by a solution-enlargement of microstylolites. In figure B, the leaching is observed to corrode a dolomite rhombohedral, indicating that the phase of leaching postdates dolomitization. Note the poor preservation of the bryozoan (to the right in Fig. B). The

zooecia walls are more and less obliterated, probably because a neomorphic alteration of both intraskeletal spar and skeleton has taken place.

Sample 136/1B. Scale of bars equal 300  $\mu\text{m}$  and 100  $\mu\text{m}$  respectively.

**Fig. T-133.** Photographs (4 : 1) of thin-section 13 6/2B showing a biosparrudite. The rock is massive, and it has a fitted fabric. Small dolomite crystals, rhombohedral in habit, are precipitated in the microstylolitic grain contacts. They are pale bluish gray coloured in the Alizarin Red S stained part of the section. The bulk of the grains are crinoid fragments, surrounded by rimcement crystals, that have been more and less truncated during the pressure solution of the rock. A: plane polarized light; B: cross polarized light.

**Fig. T-134.** Thin-section photomicrograph (plane polarized light) of bryozoan colony. It is poorly preserved, almost ghost-like in places. Intragranular, sparry calcite crystals are observed to overlie zooecia walls (arrows). We are probably dealing with a neomorphic spar. Note also the blurred boundaries between skeleton walls and spar.

Sample 13 6/2B. Scale of bar equals 100  $\mu\text{m}$ .

**Fig. T-135.** Thin-section photomicrograph (plane polarized light) of small solution vugs, formed in the microstylolitic contacts between crinoids. Some of the dolomite rhombohedrals (pale bluish coloured) are superimposed over microstylolites, indicating that the dolomite is contemporaneous with or postdates the stylolitization.

Sample 136/2B. Scale of bar equals 300  $\mu\text{m}$ .

**Fig. T-136.** Photographs (4 : 1) of thin-section 136/3. Areas of biosparrudite alternate with areas of packed biomicrudite. The rock is generally massive, even numerous small solution vugs are formed along microstylolites between grains. Arrow points to a brachiopod with geopetal micrite overlayed by sparry cement (cf. Fig. T-138).

Fig. A is photographed with plane polarized light, Fig. B with cross polarized light.

**Fig. T-137.** Thin-section photomicrographs (plane polarized light) of "packstone". Figure A shows the poorly preserved fossils, surrounded by micrite. The contacts between fossils and micrite are irregular and blurred, outer parts of fossils are replaced by micrite. A part of an area of the rock, consisting of biosparite, is seen uppermost in the picture. Arrow points to same spot in figure B. With greater magnification of the microscope, it is evident that a recrystallization of both the fossils and the surrounding lime mud has taken place, an aggrading neomorphism. The rock has now a xenotopic, sutured mosaic fabric. The calcite crystals are Axn to Vfxn in size.

Sample 136/3. Scale of bar equals 300  $\mu\text{m}$  for Fig. A, and 50  $\mu\text{m}$  for Fig. B.

**Fig. T-138.** Thin-section photomicrographs of geopetal micrite in a brachiopod shell, overlayed by sparry calcite cement. Fig. A is photographed with half-cross polarized light, Fig. B is photographed under blue-light fluorescence. The spar inside the shell (above the

geopetal micrite) is rhombohedral in habit, whereas the isopachous cement on the outer surface of the shell (lowermost in the picture) is scalenohedral in habit. The original skeletal structure of the shell is obliterated because of recrystallization, only “ghosts” of the fibrous structure are seen in places. Note that the contacts between both blocky spar and geopetal micrite, and between geopetal micrite and shell wall, are not sharp. Both the spar, the geopetal sediment, and the shell wall itself, seem to have been affected by neomorphosis. No growth zones are seen in the spar crystals in the blue-light fluorescence photograph (Fig. B), and the spar and the geopetal micrite show almost the same intensity of fluorescence. Sample 136/3. Scale of bars equal 300  $\mu\text{m}$ .

**Fig. T-139.** Photographs (4 : 1) of thin-section 136/4B, showing a faintly dolomitized biosparrudite with a fitted fabric. Numerous small solution vugs are formed in the microstylolitic grain contacts. Dissolution has in places spread from the stylolite seams into surrounding polycrystalline fossils (e.g. bryozoans), that have previously been more and less replaced by micrite. Arrows point to areas shown in Fig. T-140 and T-141. Fig. A: plane polarized light; Fig. B: cross polarized light.

**Fig. T-140.** Thin-section photomicrograph (plane polarized light) of stylolitic grain contacts between crinoids, embedded in syntaxial spar, and part of recrystallized stromatoporoid colony. Small rhombohedral dolomite crystals are precipitated in the seams. One of them is observed to overlie a seam (arrow). Some of the small solution vugs, that postdate the pressure solution, are not filled with blue-dyed resin. Sample 136/4B. Scale of bar equals 300  $\mu\text{m}$ .

**Fig. T-141.** Thin-section photomicrograph (plane polarized light) of a sparfilled bryozoan which has also been attacked by leaching. Both earlier intragranular sparry crystals and later dolomite euhedrals are more or less corroded. Note that the contacts between intragranular spar and zooecia walls are not sharp. Both the original skeletal structures and the spar seem to be neomorphic altered. Sample 136/4B. Scale of bar equals 300  $\mu\text{m}$ .

**Fig. T-142.** Photographs (4 : 1) of thin-section 136/5B, showing a biosparite to biosparrudite that has been partly replaced by dolomite. As a whole, the rock is rather massive, but several small areas with a “sucrosic texture” are dimly seen (Fig. B). Arrows point to spots, that are shown in Fig. T-144 and T-145. Fig. A is photographed with plane polarized light, and Fig. B with cross polarized light.

**Fig. T-143.** Thin-section photomicrograph (plane polarized light) of biosparite, partly replaced by a hypidiotopic dolomite spar. Sample 136/5B. Scale of bar equals 300  $\mu\text{m}$ .

**Fig. T-144.** Thin-section photomicrograph (plane polarized light) of small solution vugs formed in the microstylolitic contacts between grains. The precipitation of the numerous dolomite crystals is contemporaneous with or postdates the pressure solution of the rock, but predates the leaching, as indicated by the corrosion of many dolomite crystals. Sample 136/5B. Scale of bar equals 300  $\mu\text{m}$ .

**Fig. T-145.** Thin-section photomicrograph (half-cross polarized light) of a small area between crinoids and poorly preserved, multicrystalline fossils (bryozoans?), which has been strongly attacked by leaching. The rock shows almost a sucrosic texture here (a sieve mosaic fabric). Sample 136/5B. Scale of bar equals 300  $\mu\text{m}$ .

**Fig. T-146.** Photographs (4 : 1) of thin-section no. 136/6B show a biosparudite to packed biomicrudite that has been strongly dolomitized: about the half of the rock volume consists of sub- to euhedral dolomite crystals. Many smaller and larger solution vugs are formed along microstylolitic surfaces. The permeability of the rock is, however, probably very low as the vugs are separated from each other by massive rock; note that very little resin (blue coloured) has entered the inner part of the plug. Left arrow points to the spot shown in Fig. T-147, right arrow to the spot shown in Fig. T-148. Fig. A is taken with plane polarized light, Fig. B with cross polarized light.

**Fig. T-147.** Thin-section photomicrographs of packed biomicrite to *biomicrosparite*, resembling a packstone. The original fine-grained matrix seems to be neomorphic altered (Fig. B) - it now shows a Axn to Vfxn xenotopic sutured mosaic fabric. The skeletal grains are also affected by the neomorphism, being more and less replaced by micrite/microspar. The rhombohedral dolomite crystals are unaffected. Microstylilites are seen between many of the skeletal grains; a grain suturing, is developed during a phase of chemical compaction. Fig. A is photographed with plane polarized light, Fig. B with cross polarized light. Sample 136/6B. Scale of bars equal 300  $\mu\text{m}$  and 100  $\mu\text{m}$  respectively.

**Fig. T-148.** Thin-section photomicrograph (plane polarized light) of a rather large vug, formed by solution enlargement of microstylolitic surfaces between grains. Note that the sub- to euhedral dolomite crystals have also been attacked by leaching. Sample 136/6B. Scale of bar equals 300  $\mu\text{m}$ .

**Fig. T-149.** Photographs (4 : 1) of thin-section 136/7B show a biosparrudite to packed biomicrudite with a fitted fabric. The microstylolites between the skeletal grains are solution-enlarged. The most important grains (by volume) are crinoid fragments and some relatively large, platy grains, that resemble stromatoporoid colonies. No blue-dyed resin has entered the small vugs between the grains. The approximate direction ("up") to top of sediment, before it become lithified, is shown in Fig. A. It is indicated by the orientation of geopetal sediment in skeletons. Fig. A is photographed under plane polarized light, Fig. B under cross polarized light.

**Fig. T-150.** Thin-section photomicrograph (plane polarized light) of sparfilled coral. The irregular, serrated intercrystalline boundaries of the spar indicate that we are dealing with a neomorphic spar. That a neomorphic replacement has taken place is confirmed by the fact that corallite walls and septae have been partly obliterated. Note that some of the sparry crystals are observed to overlies the skeletal structures. Geopetal micrite/microspar is seen in some of the corallites (lowermost in the picture).  
Sample 136/7B. Scale of bar equals 3000  $\mu\text{m}$ .

**Fig. T-151.** Thin-section photomicrograph (plane polarized light) of a sparfilled vug inside a part of a stromatoporoid(?) colony. The vug was probably formed during the growth of the colony (note the small shell fragments), and later occupied by "passive" cement. Both this cement and the skeletal structure of the stromatoporoid(?) were subsequently replaced by neomorphic spar. The outline of the vug got blurred, almost ghost-like (arrows). The small non-mineralized vug (V) lowermost in the picture was eventually formed during a late-diagenetic leaching phase, postdating a phase of pressure solution.  
Sample 136/7B. Scale of bar equals 300  $\mu\text{m}$ .

**Fig. T-152.** Thin-section photomicrograph (plane polarized light) of crinoid limestone with fitted fabric. Several small, indeterminate shell fragments are also seen. Geopetal sediment occurs inside an ostracod-like fossil (arrow). A dissolution of the rock has taken place along several of the microstylolitic grain contacts.  
Sample 136/7B. Scale of bar equals 300  $\mu\text{m}$ .

**Fig. T-153.** Photographs (4 : 1) of thin-section 137/1B showing a sparse biomicrite, in places a dismicrite. Arrow points to the spot shown in Fig. T-155. Tiny solution vugs are formed along the solution seams/microstylolites, that cross the section. They are dimly seen in Fig. B. The approximate direction ("up") to top of sediment before it was lithified is shown in Fig. A (as indicated by geopetal sediment in some of the dismicritic patches).  
Fig. A: plane polarized light; Fig. B: cross polarized light.

**Fig. T-154.** Thin-section photomicrograph (plane polarized light) of bryozoans in a matrix of VFxn calcite. Note the indistinct, blurred outline of the skeletons. Both the fine-grained matrix, probably an original lime mud, and the skeletal structures have been replaced by neomorphic calcite.  
Sample 137/1B. Scale of bar equals 100  $\mu\text{m}$ .

**Fig. T-155.** Thin-section photomicrograph (plane polarized light) of "dismicrite" with an irregular patch of spar. Small, fracture-like, sparfilled structures branch off from the sparry patch. Geopetal sediment is observed to underlie the sparry patch.  
Sample 137/1B. Scale of bar equals 100  $\mu\text{m}$ .

**Fig. T-156.** Photographs (4 : 1) of thin-section 137/2B show a biolithite, a part of a stromatoporoid colony. The porosity of the rock is related to stylolites and fractures (tension gashes) that have been solution-enlarged. Arrow points to the spot shown in Fig T-157. Fig. A: plane polarized light; Fig. B: cross polarized light.

**Fig. T-157.** Thin-section photomicrographs of solution-enlarged tension gash and stylolite. Some of the rhombohedral dolomite crystals, that are precipitated along the stylolite surface, are also attacked by the leaching. Note the characteristic xenotopic sutured mosaic fabric of the stromatoporoid (Fig. B), the colony seems to have been altered during a neomorphosis. Fig. A: plane polarized light; Fig. B: cross polarized light. Sample 137/2B. Scale of bars equal 300  $\mu\text{m}$ .

**Fig. T-158.** Photographs (4 : 1) of thin-section 137/3 B of a transverse section through part of a stromatoporoid colony. A spar-filled fracture is seen to the right. The rock is massive. Fig. A: plane polarized light; Fig. B: cross polarized light.

**Fig. T-159.** Thin-section photomicrographs of a stromatoporoid colony. Original laminae appear as dusty inclusions in the calcite crystals (Fig. A), that are probably formed during a neomorphic alteration of the rock (cf. Fig. B). The fracture-like structure, crossing the picture from left to right, probably represents a temporary break of the growth of the colony. Fig A: plane polarized light; Fig. B: cross polarized light. Sample 137/3B. Scale of bars equal 300  $\mu\text{m}$ .

**Fig. T-160.** Photographs (4 : 1) of thin-section 137/4B show a rock in which areas of packed biomicrite/biomicrudite alternate with areas of biosparite/biosparrudite. Geopetal micrites (overlaid by sparry cement) in former shelter pores indicate that the direction to the top of the sediment, before it got lithified, is to the right. The rock looks massive with the naked eye, as the many solution vugs are all very small. Fig. A is photographed with plane polarized light, Fig. B with cross polarized light.

**Fig. T-161.** Thin-section photomicrograph (plane polarized light) of an ostracod shell which has been crushed during the compaction of the sediment. The shell is blurred because of micritization. The bryozoan uppermost in the picture is also very poorly preserved. A small solution vug is seen between the two fossils. A few small rhombohedral dolomite crystals are seen to the left of, and at the upper wall, of the vug. Sample 137/4B. Scale of bar equals 100  $\mu\text{m}$ .

**Fig. T-162.** Blue-light fluorescence photograph of syntaxial rimcement on crinoid fragments. Note that several rather indistinct growth zones are revealed in the cement crystals. Sample 137/4B. Scale of bar equals 100  $\mu\text{m}$ .

**Fig. T-163.** Thin-section photomicrographs showing an area between a sparfilled shelter pore and crinoid biosparite. Fig. A is taken with plane polarized light, Fig. B with blue-light fluorescence. A dissolution seam is developed here during a phase of pressure solution. Some leaching seems to have taken place later on; note the small vugs in the middle of the picture. The peculiar, dusty streaks in the sparry mosaic (in Fig. A) is probably a former geopetal mud, as indicated by the photograph taken under blue-light fluorescence (Fig. B). The coarse-grained spar is probably a neomorphic spar that has replaced the geopetal sediment. The latter appears now as ghosts in the sparry calcite crystals. Arrows point to the same spot in both figures.

Sample 137/4B. Scale of bars equals 300  $\mu\text{m}$ .

**Fig. T-164.** Photographs (4 : 1) of thin-section 137/5B show a packed biomicrudite to biosparrudite. A part of a stromatoporoid colony makes up about the half of the section. Most of the grain contacts consist of microstylolites - the rock has a fitted fabric. The direction to the top of the sediment, before it was lithified, is shown in Fig. A; it is based on the orientation of the upper surface of geopetal micrites. Arrow points to an area with geopetal sediment shown in Fig. T-166. Fig. A is photographed under plane polarized light, Fig. B under cross polarized light.

**Fig. T-165.** Thin-section photomicrograph (plane polarized light) of crinoid limestone with fitted fabric. Only very little syntaxial rimcement is seen around the crinoid fragments. Grain truncations have taken place during a phase of pressure solution.

Sample 137/5B. Scale of bar equals 300  $\mu\text{m}$ .

**Fig. T-166.** Thin-section photomicrograph (plane polarized light) showing a part of a former shelter pore, partly filled with geopetal mud (mud floor). The geopetal carbonate seems to have been replaced by neomorphic microspar, which in turn has been attacked by leaching: a sieve mosaic fabric is seen in the lower part of the sediment. The coarse-grained spar that overlays the geopetal microspar resembles a "passive" cement with plane intercrystalline boundaries. However, the very indistinct contact between the spar and the bryozoan (in the upper left corner of the picture) seems to indicate that a former "passive" cement has also been replaced by neomorphic sparry calcite.

Sample 137/5B. Scale of bar equals 300  $\mu\text{m}$ .

**Fig. T-167.** Photographs (4 : 1) of thin-section 137/6B (A: plane polarized light; B: cross polarized light), showing a biomicrudite, probably a bafflestone with bryozoans acting as baffles. No pores are seen - and not under the light microscope either. Arrow points to the sparfilled shelter pore shown in Fig. T-169.

**Fig. T-168.** Thin-section photomicrograph (plane polarized light) of the matrix of the biomicrite, that surrounds the bryozoans. Most of the *micrite* of the rock consist, in fact, of a

**Fig. T-182.** Thin-section photomicrograph (plane polarized light) of crinoid/stromatoporoid limestone with sucrosic texture. Both skeletal structures and sparry cement crystals (both of calcite and dolomite) are corroded. The microstylolitic grain contacts are still seen in many places.

Sample 139/1B. Scale of bar equals 300  $\mu\text{m}$ .

**Fig. T-183.** Thin-section photomicrograph ( $\frac{1}{2}$ -cross polarized light) of part of a stromatoporoid colony with a spar-filled fenestral pore. The neomorphic replacement, which has obliterated the skeletal structure of the stromatoporoid, has probably replaced a former "passive" cement in the fenestra. Note that the contact between the blocky spar of the fenestra and the surrounding sutured mosaic of calcite crystals in the stromatoporoid is blurred.

Sample 139/1B. Scale of bar equals 300  $\mu\text{m}$ .

**Fig. T-184.** Photographs (4 : 1) of thin-section 139/2 (plane polarized light and cross polarized light respectively). The rock is a porous biosparite, rich in both inter- and intragranular pores. Virtually all the grain contacts consist of microstylolites that have been more and less solution-enlarged.

**Fig. T-185.** Thin-section photomicrograph (plane polarized light) of porous limestone with both intergranular and intragranular porosity. The presence of almost perfect crystal faces of the crinoidal rimcement indicate that intergranular spaces have not been filled totally by rimcement crystals, that have later been partly dissolved. Residuals inside the rimcement (arrow) seem to indicate that the rimcement has grown at the expense of bryozoan skeletal structure with associated isopachous cement.

Sample 139/2. Scale of bar equals 300  $\mu\text{m}$ .

**Fig. T-186.** Thin-section photomicrograph (plane polarized light) of crinoidal rimcements that seem to have partly replaced bryozoan skeleton with associated isopachous cement, scalenohedral in habit.

Sample 139/2. Scale of bar equals 300  $\mu\text{m}$ .

**Fig. T-187.** Photographs (4 : 1) of thin-section 139/3B (A: plane polarized light; B: cross polarized light) show a porous biosparite. A few granule sized grains of crinoids are also seen. Note that most of the numerous intergranular pores have not been filled with blue-dyed resin, indicating that the rock is probably a little less permeable than the rock of sample 139/2. The rock has a well-developed fitted fabric.

**Fig. T-188.** Thin-section photomicrograph (plane polarized light) of a rectangular to sutured type of stylolite, which is formed locally in the rock with fitted fabric. The dentate surface is only a few mm long, when seen in cross section. A leaching has strongly attacked the rock after the stylolitization took place.

Sample 139/3B. Scale of bar equals 300  $\mu\text{m}$ .



**Fig. T-189.** Photographs (4 : 1) of thin-section 139/4 (A: plane polarized light; B: cross polarized light) show a porous biosparite to biosparudite with fitted fabric. Note that most of the numerous inter- and intragranular pores have not been occupied by blue-dyed resin (cf. sample 139/3 B in Fig. T-187).

**Fig. T-190.** Thin-section photomicrograph (plane polarized light) of limestone with a sieve-mosaic-like fabric. The fossils with associated cements are strongly attacked by a leaching, which took place after a phase of pressure solution, resulting in a fitted rock fabric (cf. the rock of sample 139/2 shown in Fig. T-185).  
Sample 139/4. Scale of bar equals 300  $\mu\text{m}$ .

**Fig. T-191.** Photographs (4 : 1) of thin-section 139/5B (A: plane polarized light; B: cross polarized light) of a biosparudite with fitted fabric. Two massive, tabulate corals make up about the half of the thin-section. The remaining part of the section consist of a porous biosparite with numerous inter- and intragranular pores. Note that most of the pores are filled in with blue-dyed resin, indicating that the rock has here a rather high permeability.

**Fig. T-192.** Thin-section photomicrograph ( $\frac{1}{2}$ -cross polarized light) of crinoid rimcement which seems to have partly replaced some of the scalenohedral cement crystals on a poorly preserved fossil fragment (arrows), cf. Fig. T-185 and T-186. The crinoid fragment itself (uppermost in the picture) is preserved as dusty inclusions, embedded in the syntaxial rimcement.  
Sample 139/5B. Scale of bar equals 100  $\mu\text{m}$ .

**Fig. T-193.** Thin-section photomicrograph (plane polarized light) of a part of a tabulate coral that has been neomorphic altered. The blocky spar of the corallites (between the partly obliterated septae and tabulae) is not a "passive" cement, as some of the sparry crystals are observed to overlie the skeletal structure (arrows). An older isopachous cement, scalenohedral in habit, is dimly seen, being almost ghost-like.  
Sample 139/5B. Scale of bar equals 300  $\mu\text{m}$ .

**Fig. T-194.** Photographs (4 : 1) of thin-section 139/6B (A: plane polarized light; B: cross polarized light) of a porous biosparite with fitted fabric.

**Fig. T-195.** Thin-section photomicrograph (plane polarized light) of crinoid limestone with fitted fabric. A phase of leaching postdates the phase of chemical compaction, as indicated by the presence of small solution vugs, that are formed in the stylolitic grain contacts.  
Sample 139/6B. Scale bar equals 300  $\mu\text{m}$ .

**Fig. T-196.** Thin-section photomicrograph (plane polarized light) of intergranular cement. The thin coat of isopachous cement (scalenohedral in habit) on the shell fragment has been partly undercut by leaching. The shell itself, probably a poorly preserved brachiopod, is broken, the small fissure being solution-enlarged. The presence of isopachous cement of small dentate crystals at the contact between shell fragment and large syntaxial rimcement (on crinoid), see the arrow, indicates that the rimcement was precipitated after the precipitation of the isopachous cement (cf. the passage concerning diagenetic considerations in the description of sample 139/2).

Sample 139/6B. Scale of bar equals 100  $\mu\text{m}$ .

**Fig. T-197.** Photographs (4 : 1) of thin-section 139/7B (A: plane polarized light; B: cross polarized light) showing a very porous biosparite to biosparrudite with fitted fabric, probably an original lime sand in which the interstitial spaces have only been partly filled in by sparry calcite cement.

**Fig. T-198.** Thin-section photomicrograph (plane polarized light) showing a biosparite which has been strongly attacked by leaching; both the fossils (mostly crinoid fragments) and the sparry calcite cement are affected. Small pores in sutured grain contacts indicate that the leaching took place after a phase of chemical compaction. The subhedral dolomite crystals (arrow), that are precipitated contemporaneously with or after the chemical compaction, are also attacked by leaching.

Sample 139/7B. Scale of bar equals 300  $\mu\text{m}$ .

**Fig. T-199.** Thin-section photomicrograph (plane polarized light) of a relatively well-developed microstylolite, formed around a large stromatoporoid (lowermost in the picture). Note how the stromatoporoid colony has been partly dissolved along the stylolite surface. The crinoid fragments and the bryozoan (above the stromatoporoid) with associated sparry calcite cements have also been partly dissolved during the same phase of leaching.

Sample 139/7B. Scale of bar equals 300  $\mu\text{m}$ .